JOURNAL OF BACTERIOLOGY, Jan. 2001, p. 309–317 Vol. 183, No. 1
0021-9193/01/$04.00+0 DOI: 10.1128/JB.183.1.309–317.2001

Vibrio fischeri Genes *hvnA* and *hvnB* Encode Secreted NAD^+-Glycohydrolases

ERIC V. STABB,[1]* KARL A. REICH,[2]† AND EDWARD G. RUBY[1]

Pacific Biomedical Research Center, University of Hawaii, Honolulu, Hawaii 96813,[1] and Department of Microbiology and Immunology, Stanford University School of Medicine, Stanford, California 94305[2]

Received 22 June 2000/Accepted 27 September 2000

HvnA and HvnB are proteins secreted by *Vibrio fischeri* ES114, an extracellular light organ symbiont of the squid *Euprymna scolopes*, that catalyze the transfer of ADP-ribose from NAD^+ to polyarginine. Based on this activity, HvnA and HvnB were presumptively designated mono-ADP-ribosyltransferases (ARTases), and it was hypothesized that they mediate bacterium-host signaling. We have cloned *hvnA* and *hvnB* from strain ES114. *hvnA* appears to be expressed as part of a four-gene operon, whereas *hvnB* is monocistronic. The predicted HvnA and HvnB amino acid sequences are 46% identical to one another and share 44% and 34% identity, respectively, with an open reading frame present in the *Pseudomonas aeruginosa* genome. Four lines of evidence indicate that HvnA and HvnB mediate polyarginine ADP-ribosylation not by ARTase activity, but indirectly through an NAD^+-glycohydrolase (NADase) activity that releases free, reactive, ADP-ribose: (i) like other NADases, and in contrast to the ARTase cholera toxin, HvnA and HvnB catalyzed ribosylation of not only polyarginine but also polylysine and polyhistidine, and ribosylation was inhibited by hydroxylamine; (ii) HvnA and HvnB cleaved 1,N^6-etheno-NAD^+ and NAD^+; (iii) incubation of HvnA and HvnB with [^{32}P]NAD^+ resulted in the production of ADP-ribose; and (iv) purified HvnA displayed an NADase V_{max} of 400 mol min^{-1} mol^{-1}, which is within the range reported for other NADases and 10^2- to 10^4-fold higher than the minor NADase activity reported in bacterial ARTase toxins. Construction and analysis of an *hvnA hvnB* mutant revealed no other NADase activity in culture supernatants of *V. fischeri*, and this mutant initiated the light organ symbiosis and triggered regression of the light organ ciliated epithelium in a manner similar to that for the wild type.

The light organ symbiosis between *Vibrio fischeri* and the Hawaiian bobtail squid, *Euprymna scolopes*, is a stable, benign bacterial colonization of host tissue in which both partners recognize, signal, and influence the other (48). *V. fischeri* triggers developmental changes in the tissues of this organ, including apoptosis, cell swelling, microvillar proliferation, and repression of oxidative stress (11, 27, 31, 34, 38, 51), sparking interest in discovering the molecular mechanisms mediating this signaling. Two proposed signaling molecules are halovibrin α (HvnA) and halovibrin β (HvnB), proteins secreted by *V. fischeri* (46, 47). HvnA and HvnB catalyzed transfer of ADP-ribose (ADPr) from NAD^+ to the synthetic polypeptide polyarginine (46, 47), a reaction catalyzed by certain secreted bacterial mono-ADP-ribosyltransferase (ARTase) toxins (e.g., cholera toxin) that interact with host tissues. These data led to speculation that HvnA and HvnB mediate symbiotic signaling through mechanisms that parallel ARTase toxin modification of host targets (32, 33, 46, 47, 49).

To assess the potential role(s) of HvnA and HvnB as interspecies signals, the nature of HvnA- and HvnB-catalyzed ribosylation requires clarification. Although HvnA and HvnB catalyze the transfer of radiolabel from [^{32}P]NAD^+ to polyarginine (46, 47), either of two distinct classes of enzymes, ARTases and NAD^+-glycohydrolases (NADases), can mediate this process. ARTases directly ribosylate protein targets, often at an arginine residue, using NAD^+ as a substrate. In contrast, NADases cleave NAD^+, producing free nicotinamide and ADPr, the latter of which spontaneously forms covalent bonds with a variety of substrates (21, 22, 26), including polyarginine (21). Thus, the assay used to identify HvnA and HvnB did not distinguish between ARTase or NADase activity. Secreted bacterial ARTases clearly mediate defined effects on certain animal host cells (15, 39–41), but the role, if any, of secreted NADases in bacterium-host interactions is unknown beyond the observations that clinical streptococcal isolates and *Vibrio cholerae* secrete NADases (24, 52).

We present here (i) the characterization of *hvnA* and *hvnB* from an *E. scolopes* light organ isolate, (ii) the disruption of these genes in this wild-type *V. fischeri* strain, (iii) biochemical data supporting a reclassification of HvnA and HvnB as NADases rather than as ARTases, and (iv) evidence that HvnA and HvnB are not required to initiate the *V. fischeri-E. scolopes* symbiosis.

MATERIALS AND METHODS

Bacteria, media, and reagents. Wild-type *V. fischeri* ES114, isolated from *E. scolopes* (3), was the parent strain for mutant construction and was the source of DNA for the cloning of *hvnA* and *hvnB*. *Escherichia coli* strains DH5α (16) and BW23474 (14) were used as hosts for plasmids with ColE1 or R6K replication origins, respectively, with the exception of plasmid pUTminiTn*5*-Sm/Sp, which was maintained in strain CC118λ*pir* (19). *E. coli* was grown in Luria-Bertani (LB) medium (36), and *V. fischeri* was grown in either SWT medium (3) or LBS medium, which contained, per liter of water, 10 g of tryptone, 5 g of yeast extract, 20 g of NaCl, and 20 mM Tris-hydrochloride (Tris) (pH 7.5).

All chemicals were obtained from Sigma Chemical Co. (St. Louis, Mo), except [α-^{32}P]NAD^+ (1 Ci/μmol), which was obtained from Amersham Pharmacia

* Corresponding author. Mailing address: Pacific Biomedical Research Center, University of Hawaii, 41 Ahui St., Honolulu, HI 96813. Phone: (808) 539-7311. Fax: (808) 599-4817. E-mail: stabb@hawaii.edu.

† Present address: Abbott Laboratories, Abbott Park, IL 60064.

Biotech (Piscataway, N.J.). Restriction enzymes and DNA ligase were obtained from New England Biolabs (Beverly, Mass.). AmpliTaq DNA polymerase was obtained from Perkin-Elmer (Branchburg, N.J.). Oligonucleotides were synthesized by Operon Technologies, Inc. (Alameda, Calif.). When added to LB medium for the selection of *E. coli*, ampicillin, trimethoprim, chloramphenicol, streptomycin, and kanamycin were used at concentrations of 100, 20, 20, 100, and 40 μg ml^{-1}, respectively. When added to LBS medium for selection in *V. fischeri*, trimethoprim, chloramphenicol, streptomycin, and kanamycin were used at concentrations of 5, 5, 200, and 100 μg ml^{-1}, respectively.

Cloning, sequence analysis, and disruption of *hvnA* and *hvnB*. *hvnB* was cloned using hybridization techniques and a DNA probe based on a partial peptide sequence of HvnB. HvnB was purified as described previously (46) and subjected to in-gel trypsin digestion, and peptides were separated by reversed-phase high-pressure liquid chromatography, prior to peptide sequencing (Beckman Center Protein and Nucleic Acid Facility, Stanford, Calif.). Based on this partial HvnB amino acid sequence, an oligonucleotide (5′-GGT GGA GTT TCC TTC TCT TAC CTT CGT ACA GAT ACT AAA TTT TCG AGA TTA GCT TAT GG-3′) was designed, end labeled with digoxigenin (DIG Oligonucleotide Tailing Kit; Boehringer Mannheim), and used in Southern and dot blotting experiments (DIG DNA Labeling and Detection Kit; Boehringer Mannheim) to identify *hvnB*-containing DNA fragments. Blots were hybridized with the probe overnight at 32°C, membranes were washed under low-stringency conditions (two 30-min washes in 30 mM sodium citrate–300 mM NaCl–0.1% sodium dodecyl sulfate [SDS] [pH 7.0] at 42°C) prior to development, according to the manufacturer's instructions. A 3.9-kb *Xba*I fragment containing *hvnB* was identified, gel purified, and cloned into the *Xba*I site in pBC SK (Stratagene, Inc., La Jolla, Calif.) generating pEVS47, which was subcloned by digestion with *Eco*RV and self-ligation to form pEVS47EV. pEVS47EV was mutagenized with miniTn*5*-Sm/Sp (19), and transposon insertions were mapped by sequencing. An insertion interrupting codon 73 of the HvnB open reading frame (ORF) was identified and, along with 1.3 kb of flanking *V. fischeri* chromosomal DNA extending in each direction, was cloned into the mobilizable suicide vector, pEVS54, generating pEVS57. pEVS54 is a derivative of pKNG101 (23) with a trimethoprim resistance determinant replacing streptomycin resistance. pEVS57 was used to replace the chromosomal *hvnB* allele in strain ES114 with *hvnB*::miniTn*5*-Sm/Sp by marker exchange (see below).

hvnA was cloned using PCR to screen an existing library (55) of *Eco*RI-digested ES114 genomic DNA cloned in pBluescript KS (Stratagene, Inc., La Jolla, Calif.). PCR reactions were prepared as previously described (8) and subjected to either 35 or 40 cycles consisting of 94°C for 1.75 min, 45°C for 2 min, and 72°C for 4 min, followed by a single 72°C incubation for 10 min. The primers used were the M13 reverse primer (Stratagene) and 5′-AGT GGT GGA GTT TCC TTC TCT TAC C-3′. Using PCR to identify *hvnA* in increasingly smaller pools of clones, we isolated plasmid pEVS30, which carries *hvnA* on an 8.7-kb *Eco*RI fragment. Sequencing this insert revealed identity between this copy of *hvnA* and the *hvnA* previously cloned from a fish light organ symbiont. Therefore, the mobilizable suicide plasmid pKNG101/L+R/*cat*, which contains an *hvnA* knockout construct generated from the fish symbiont sequence (46), was appropriate for the construction of *hvnA*-null mutants in ES114 by marker exchange (see below). The *Sal*I fragment of pKNG101/L+R/*cat*, which contains the *hvnA* knockout construct and flanking chromosomal DNA, was cloned into the unique *Sal*I site in pEVS54 to generate pEVS61, which was used to introduce the *hvnA*-null allele into an *hvnB*::miniTn*5*-Sm/Sp mutant by marker exchange.

Mutant (null) *hvnA* and *hvnB* alleles (described above) were introduced into the ES114 chromosome by marker exchange. Mobilizable suicide vectors were transferred to ES114 by triparental mating, using pRK2013 (9) as a conjugal helper plasmid. *E. coli* donor strains and *V. fischeri* ES114 were grown to mid-log phase, pelleted, washed with antibiotic-free medium, pelleted again, suspended in 15 μl of LBS medium, dropped on LBS agar plates, incubated for 16 h at 28°C, transferred to LBS liquid medium, and plated on antibiotic-containing LBS agar. These plates were incubated at 22°C to enrich for *V. fischeri*, which rapidly outgrows *E. coli* donors at this temperature. The addition of chloramphenicol (pKNG101/L+R/*cat* and pEVS61) or streptomycin (pEVS57) enabled selection of single-recombinant events between the mobilized, nonmaintained, plasmids and the ES114 genome. Double recombinants that had lost vector sequences were identified by screening for loss of resistance to trimethoprim (pEVS61 and pEVS57) or streptomycin (pKNG101/L+R/*cat*) following nonselective growth. Double recombinants arose at frequencies of approximately 10^{-2} (pEVS57) or 10^{-3} (pKNG101/L+R/*cat* and pEVS61). Double recombinants that retained the antibiotic resistance determinants of mutant *hvnA* or *hvnB* alleles were examined by Southern blotting to verify the chromosomal replacement of wild-type *hvnA* and *hvnB* with the knockout constructs. Strains EVS498, EVS499, and EVS500, were chosen as representative *hvnA*, *hvnB*, and *hvnA hvnB* mutant derivatives of ES114, respectively.

Plasmids were purified using the PerfectPrep plasmid DNA kit (5 Prime-3 Prime, Inc., Boulder, Colo.). Between restriction and ligation reactions DNA was recovered with the Wizard DNA Cleanup System (Promega Corp., Madison, Wis.). DNA sequencing was conducted on an ABI automated DNA sequencer at the University of Hawaii Biotechnology/Molecular Biology Instrumentation and Training Facility. Both strands of each insert were sequenced. Sequence analysis (e.g., the identification of ORFs and putative stem-loops) was performed using DNA Strider 1.2, and comparisons of ORF and protein sequences were conducted with either the CLUSTAL W (53) or the BLASTP (1) algorithms, using the BLOSUM62 scoring matrix (17).

Enzyme assays. Enzyme assays were performed at 30°C in sodium phosphate (SP) buffer, (25 mM, pH 7.0), with 20 mM dithiothreitol (DTT), in 100 μl of total volume. Assays of HvnA kinetic properties were performed as above, except the buffer contained 2 mM DTT and 100 μg of bovine serum albumin per ml. To assess secreted enzyme activity of wild-type and mutant *V. fischeri*, overnight cultures were diluted 300-fold and grown for 15 h in LBS medium at 28°C, cells were pelleted, and culture supernatants were passed through 0.2-μm-pore-size filters; 15 μl of filtrate was then added directly to the ADPr transfer assays.

To assess its kinetic properties, a sample of HvnA that was at least 95% pure (as determined by SDS-polyacrylamide gel electrophoresis [PAGE]) was prepared as follows. The cloned *hvnA*-containing *Eco*RI fragment (see above and Fig. 1) was subcloned into shuttle vector pVO8 (54), generating pPFhvnA, which was conjugally mobilized into the *hvnB* mutant strain EVS499. The resulting strain displayed an approximately 25-fold increase in HvnA activity in culture supernatants relative to untransformed EVS499. HvnA was harvested from culture filtrates of EVS499 pPFhvnA by stepwise $(NH_4)_2SO_4$ precipitation. Proteins precipitated by 277 g of $(NH_4)_2SO_4$ per liter were discarded, and HvnA was precipitated by subsequent addition of $(NH_4)_2SO_4$ up to 390 g $liter^{-1}$. HvnA was concentrated, desalted, and dialyzed against 20 mM Tris (pH 7.9) using Centriprep 30 ultrafiltration apparati (Amicon/Millipore, Inc., Bedford, Mass.), which retained HvnA. Large proteins and protein complexes were removed using Centricon YM100 (Amicon/Millipore, Inc.), which retained <10% of the HvnA activity. Proteins in the YM100 filtrate were separated by fast-protein liquid chromatography, using a MonoQ HR5/5 column (Pharmacia Biotech, Piscataway, N.J.), a 1-ml min^{-1} flow rate, and a gradient from 0 to 500 mM NaCl. Proteins were detected as they eluted by measuring the absorbance at 280 nm (Hewlett-Packard series 1100), and individual peaks were collected. HvnA eluted at approximately 110 mM NaCl. At each step in the purification, HvnA-containing fractions were identified by assaying for 1,N^6-etheno-NAD^+ (ε-NAD^+) degradation (see below). The rate of HvnA-mediated NAD^+ hydrolysis was determined (see below) using 25 ng of purified HvnA and 400, 200, 133, 100, 67, or 50 μM NAD^+.

To assess HvnA and HvnB activity in the presence of other secreted proteins, filtrates were concentrated and then separated from small solutes (<10 kDa) using Centricon YM10 (Amicon/Millipore, Inc.). Ten milliliters of culture filtrate was concentrated to 300 μl and then subjected to three sixfold washes in SP buffer. Cholera toxin and NADase enzymes were maintained as 1-mg ml^{-1} stock solutions and diluted in reaction buffer immediately prior to addition.

Assays of ADPr transfer from NAD^+ were performed as described elsewhere (47), except that 100-μl reactions were spotted onto 2.3-cm filter disks soaked in 10% trichloroacetic acid (TCA) and washed four times with 5 ml of 5% TCA using a vacuum manifold. Polyarginine, polylysine, and polyhistidine were added to a final concentration of 1 mg ml^{-1}. Hydroxylamine-HCl was neutralized with NaOH prior to use. NAD^+ concentrations were assayed by the addition of KCN (667 mM, final concentration), measurement of absorbance at 340 nm and comparison to a standard curve (2, 5). ε-NAD^+ degradation was monitored by measuring the increase in fluorescence at 465 nm of samples excited with a 340-nm-wavelength light. Measurements of NAD^+ and ε-NAD^+ degradation were performed on a Perkin-Elmer HTS7000 fluorimeter. Thin-layer chromatography (TLC) was performed after 1-h incubations of samples with [^{32}P] NAD^+. A 5-μl portion of each reaction was spotted onto TLC plates and developed in one of three solvent systems: (i) Cellulose 300 plates (Selecto Scientific) and isobutyrate-H_2O-NH_4OH (96:19:4, vol/vol/vol) running buffer (13), (ii) silica plates (PE SIL G/UV; Whatman, Ltd., Maidstone, Kent, England) with H_2O-ethanol-NaCl (30%:70%:0.2 M) solvent, or (iii) silica plates with H_2O-ethanol-NH_4HCO_3 (30%:70%:0.2 M) solvent (20). Plates were dried and developed by autoradiography. ADPr was added as a standard and visualized under UV light. ADPr cyclase from *Aplysia californica* was incubated with [^{32}P] NAD^+ to generate a cADPr standard. In each TLC system, NAD^+, ADPr, and cADPr displayed relative mobilities similar to those previously reported (13, 20).

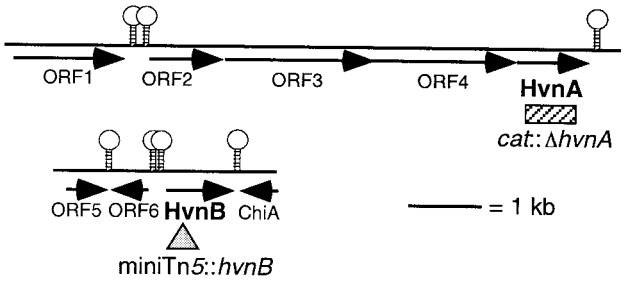

FIG. 1. Sequence analysis of *hvnA* and *hvnB* clones. Solid lines, arrows, and stem-loops represent *V. fischeri* genomic DNA, ORFs, and putative intergenic Rho-independent transcriptional terminators, respectively. The hatched rectangle corresponds to the region deleted and replaced by the chloramphenicol acetyltransferase (*cat*) gene in strains EVS498 and EVS500. The shaded triangle indicates the position of the miniTn*5*-Sm/Sp insertion recombined into the chromosomes of strains EVS499 and EVS500. These sequence data have been submitted to the GenBank database under accession numbers AF206719 and AF206718 for the *hvnA*- and *hvnB*-containing clones, respectively.

Symbiosis assays. The ability of *V. fischeri* strains to initiate colonization of the *E. scolopes* light organ was measured as described previously (50). Juvenile *E. scolopes* organisms were inoculated in the evening, within 3 h after hatching. Regression of the light organ ciliated epithelial appendages was examined using scanning electron microscopy (SEM) as described elsewhere (37), except that animals were treated with 1% osmium tetroxide in 0.1 M sodium cacodylate (pH 7.4) after fixation in 4% formaldehyde. Examination of light organ crypt epithelial cells was performed by transmission electron microscopy (TEM) as described previously (11), but without uranyl acetate treatment.

RESULTS

The goals of this study were (i) to clone *hvnA* and *hvnB* from an *E. scolopes* isolate of *V. fischeri*, (ii) to determine whether an *hvnA hvnB* double mutant possesses any other extracellular Hvn-like activity, (iii) to test whether HvnA- and HvnB-catalyzed ribosylation of polyarginine is mediated directly by an ARTase activity or indirectly by NADase activity, and (iv) to determine whether an *hvnA hvnB* double mutant is capable of colonizing and triggering development of the *E. scolopes* light organ.

Cloning of *hvnA* and *hvnB*. *hvnA* and *hvnB* were cloned from the squid light organ isolate ES114. The *hvnA* gene from ES114 was identical to *hvnA* previously cloned from the fish light organ isolate, *V. fischeri* MJ1, although there were minor differences in nearby ORFs (see below). Because the amino acid sequence derived from the *hvnB* gene matched peptide sequences within the HvnB protein and because the derived molecular mass (35 kDa) approximated the 32 kDa deduced for HvnB by gel electrophoresis (46), we concluded that this cloned gene encoded HvnB. Based on the location and orientation of the ORFs, the gaps between ORFs, and the location of putative transcriptional terminators, *hvnA* appears to be part of a four-gene operon, whereas *hvnB* is monocistronic (Fig. 1). None of the ORFs upstream of, and putatively cotranscribed with, *hvnA* showed convincing similarity to known proteins, although short (50 to 179 amino acid) stretches of ORF3 and ORF4 were 43 to 60% similar to certain bacterial outer membrane proteins, including the enteric flagellar hook protein FlgE (ORF3) and the *Haemophilus influenzae* filamentous adhesin Hmw2A (ORF4). There were minor variations between strains ES114 and MJ1 in ORF3 and ORF4, amounting to 1.3 and 0.1% nonidentity, respectively. The ORF immediately downstream of *hvnB* displayed 30% identity and 50% similarity to chitinase A of *Vibrio harveyi*. ORF5 and ORF6, upstream of *hvnB*, were similar to YKGJ and YGJP, genetically unlinked ORFs of unknown function in *E. coli*.

The HvnA and HvnB sequences derived from their respective genes are 46% identical to one another, share 44% and 34% identity, respectively, with an ORF present in the *Pseudomonas aeruginosa* genome, and contain regions that are similar to a 47-amino-acid stretch in human nicotinamide nucleotide transhydrogenase (Fig. 2). No other significant similarities were observed in protein database searches, suggesting that HvnA, HvnB, and the ORF in *P. aeruginosa* comprise a new protein family.

Absence of secreted ADP-ribosylating activity in an *hvnA* and *hvnB* double mutant. Null mutant derivatives of *hvnA* and *hvnB* were constructed singly and in tandem by marker exchange in wild-type *V. fischeri* ES114. The chloramphenicol acetyltransferase gene replaced a deleted portion of *hvnA* in strains EVS498 and EVS500, and a miniTn*5*-Sm/Sp insertion was used to interrupt *hvnB* in strains EVS499 and EVS500 (Fig. 1). Construction of these mutants was confirmed by Southern blotting (data not shown). To test whether a third secreted Hvn-like activity was present in *V. fischeri*, culture supernatants of ES114, EVS498, EVS499, and EVS500 were tested for their ability to catalyze ribosylation of polyarginine. The single mutants EVS498 and EVS499 showed activity levels similar to that of ES114 (Fig. 3). Although we initially expected intermediate activities from the single mutants, the data in Fig. 3 are consistent with a model (see below) wherein HvnA and HvnB have high NADase activity, quickly hydrolyzing the [^{32}P]NAD$^+$ to [^{32}P]ADPr, with subsequent nonenzymatic incorporation of label onto the polyarginine substrate. The double mutant EVS500 showed no detectable activity above background (Fig. 3), and supernatant-mixing experiments revealed no anti-Hvn activity secreted by EVS500 (data not shown). Based on these data, there does not appear to be a third Hvn-like protein expressed and secreted by *V. fischeri* ES114 in culture, and the ribosylating activities of EVS498 and EVS499 are presumably solely due to HvnB and HvnA, respectively.

NADase activity of HvnA and HvnB. Because ADP-ribosylation of polyarginine can be mediated either directly by ARTase activity or indirectly by NADase activity (21), we tested the enzymatic nature of HvnA and HvnB. Ribosylation mediated by NADase activity occurs via a free ADPr intermediate, which reacts spontaneously with polyarginine, polylysine, polyhistidine, hydroxylamine, or a number of other molecules (21, 22, 26). In contrast, ARTases are relatively target specific. *Neurospora crassa* NADase and the bifunctional ADPr cyclase/cADPr-hydrolase of *A. californica*, both of which generate free ADPr from NAD$^+$, each catalyzed the ribosylation of polyarginine, polylysine, and polyhistidine (Fig. 4). For these enzymes, ribosylation of polyarginine could be inhibited with 10 mM hydroxylamine, which scavenges free ADPr (Fig. 4). In contrast, the ARTase cholera toxin catalyzed the ribosylation of polyarginine in a hydroxylamine-insensitive manner but did not catalyze the ribosylation of either polylysine or polyhistidine (Fig. 4). Although 1 M hydroxylamine can slowly remove ADPr from ribosylated arginine residues (44), the hydroxyl-

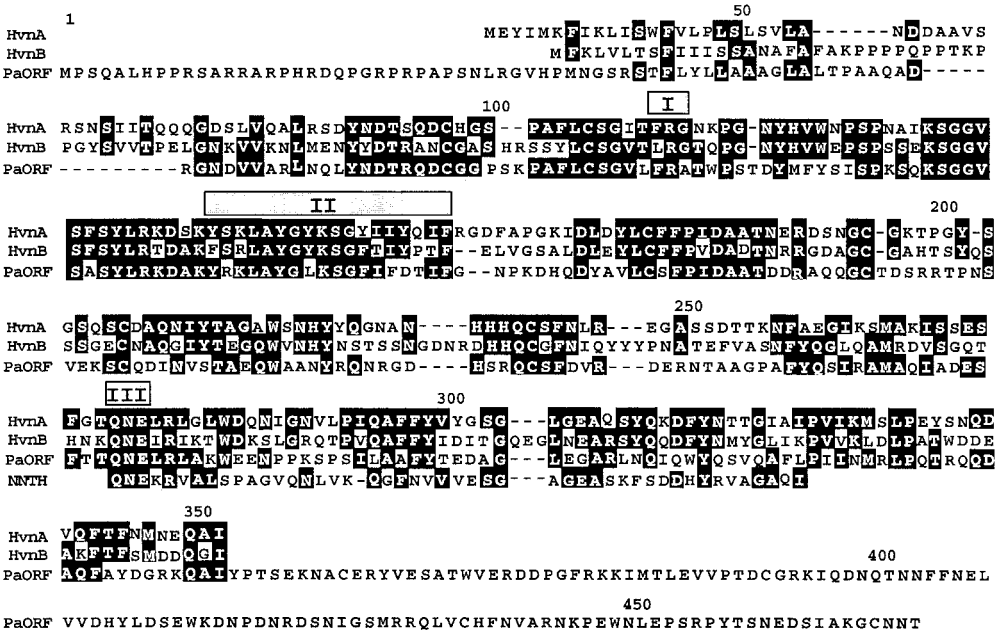

FIG. 2. Sequence comparison of HvnA and HvnB. Amino acid alignment of HvnA, HvnB, an ORF present in the *P. aeruginosa* genome, indicated by PaORF, and residues 67 to 113 of the human nicotinamide nucleotide transhydrogenase, indicated by NNTH. Identical aligned residues are indicated by white letters on black background. Dashes indicate gaps introduced into the sequence to facilitate alignment. Shaded boxes are aligned above segments with similarity to regions I, II, and III, which are conserved among ARTases and NADases (see Discussion) (43).

amine insensitivity of cholera toxin activity demonstrates that, under these conditions, hydroxylamine did not significantly disrupt ADPr-arginine bonds formed by ARTase activity. ADPr transfer catalyzed by HvnA and HvnB was consistent with a reaction mediated by a free ADPr intermediate, because ribosylation of polyarginine was hydroxylamine sensitive, and ribosylation of polylysine and polyhistidine was also catalyzed (Fig. 4). Therefore, in this assay, HvnA and HvnB catalyzed reactions consistent with NADase activity and inconsistent with ARTase activity. We considered the possibility that other secreted proteins might be required for ARTase activity by HvnA or HvnB, but that does not seem to be the case because these experiments were performed with preparations that included other proteins secreted by *V. fischeri*. Similar results were obtained with purified HvnA, which ribosylated polyarginine, polylysine, and polyhistidine, each in a hydroxylamine-sensitive manner (data not shown).

If the first step in HvnA- and HvnB-mediated ADP-ribosylation of polyarginine is the breakdown of NAD^+; then these enzymes should degrade NAD^+ in the absence of a polypeptide target. Several lines of evidence suggest that this degradation occurs. First, HvnA and HvnB each catalyzed the degradation of ε-NAD^+, an NAD^+ analog whose fluorescence increases when the ADP moiety is released from the fluorescence-quenching nicotinamide (Fig. 5A). These data are consistent with HvnA and HvnB possessing NADase activity; however, the reaction of ε-NAD^+ with phosphodiesterase and NAD^+ pyrophosphatase activities also results in an increase in fluorescence (13). In a second assay, the breakdown of NAD^+ was measured by the addition of cyanide, which forms a light-absorbing complex with N-substituted nicotinamide compounds (5), allowing detection of nicotinamide-ADPr bond cleavage. We found that NAD^+ is degraded by HvnA and HvnB, indicating that these enzymes cleave the nicotinamide-ribose bond of NAD^+ (Fig. 5B).

The data presented in Fig. 4 and 5 suggested that the cleavage of NAD^+ by HvnA and HvnB produced free ADPr; how-

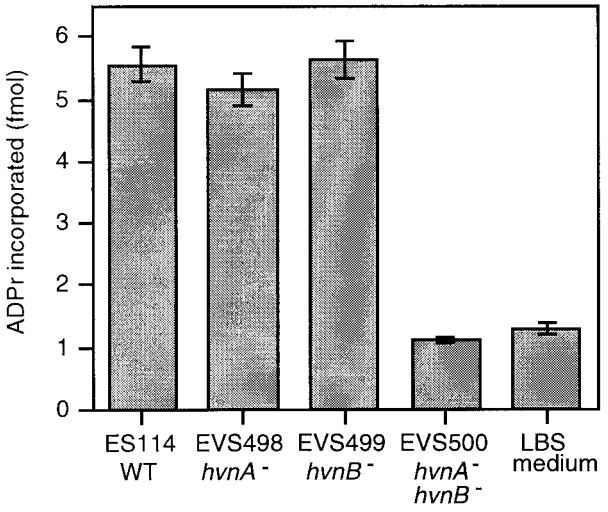

FIG. 3. Transfer of ADPr to polyarginine catalyzed by *V. fischeri* halovibrin mutants. Culture supernatants from strain ES114 (wild type), the EVS498 *hvnA*, EVS499 *hvnB*, and EVS500 *hvnA hvnB* mutant strains, and an LBS medium control were filtered and incubated with [^{32}P]NAD^+ and polyarginine. Polyarginine was precipitated on TCA-soaked filters, which were washed and assayed for radiolabel incorporation into macromolecules. ADPr incorporation was calculated from the counts per minute, assuming that the radiolabel detected corresponds to recovery of the ADPr moiety from [^{32}P]NAD^+. Error bars (too small to visualize in the EVS500 treatment) indicate standard errors (n = 3).

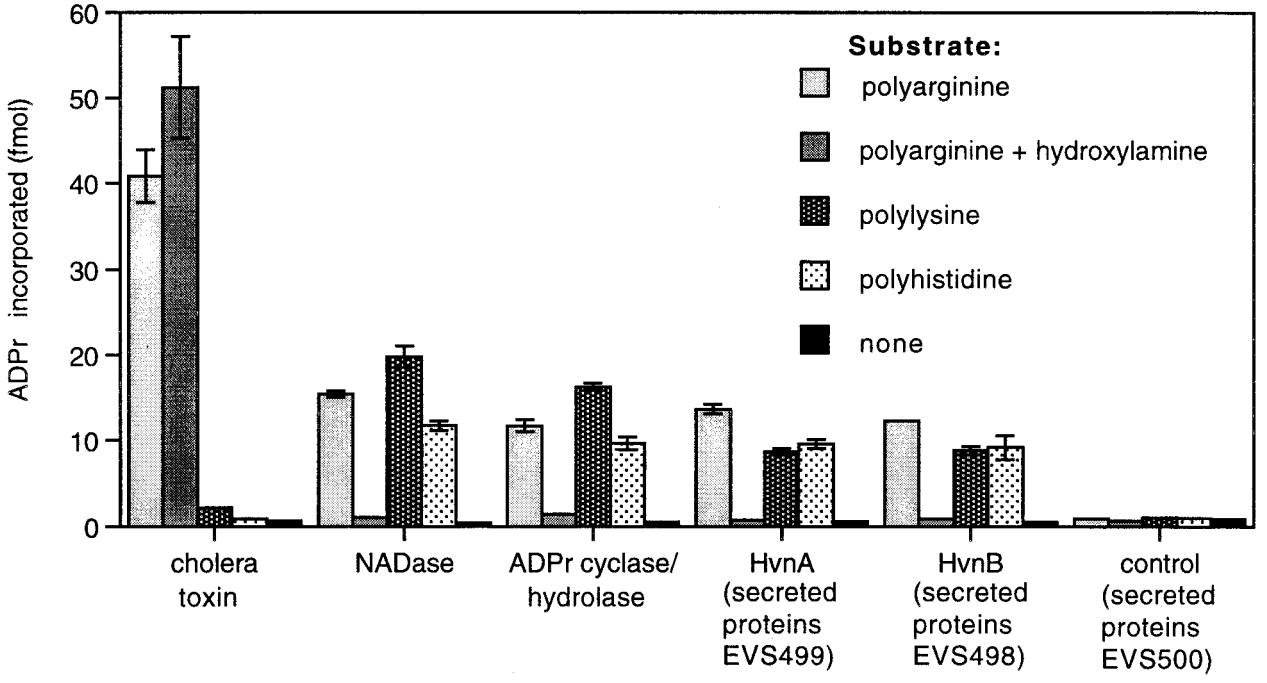

FIG. 4. Ribosylation patterns of HvnA and HvnB. Transfer of ADPr to polyamino acids was measured for cholera toxin (75 ng), *N. crassa* NADase (300 ng), *A. californica* ADPr cyclase-cADPr hydrolase (~75 ng), HvnA, and HvnB. HvnA and HvnB were added as dialyzed preparations of total secreted proteins by strains EVS499 and EVS498, respectively. A secreted protein preparation from strain EVS500 was a negative control. The amounts of HvnA, HvnB, and control preparations corresponded to 15 μl of culture supernatant. Enzymes were incubated with [^{32}P]NAD$^+$ and polyarginine, polylysine, or polyhistidine or no polyamino acid substrate (none) as indicated. Parallel reactions with polyarginine were supplemented with 10 mM hydroxylamine. Polyamino acids were precipitated on TCA-soaked filters, which were washed and assayed for radiolabel incorporation. ADPr incorporation was calculated as in Fig. 3. Error bars (often too small to visualize) indicate standard errors (n = 3).

ever, these results were also consistent with a different hydrolysis product, such as cADPr. Using TLC with three different mobile-phase–stationary-phase combinations, we determined that ADPr was the major product of HvnA- and HvnB-mediated NAD$^+$ breakdown (Fig. 6 and data not shown), confirming that HvnA and HvnB catalyze an NADase reaction.

Most ARTases possess minor NADase activity; however, NADases typically possess specific activities higher than the low residual NADase activity inherent in ARTases. To test whether halovibrin NADase activity resembled that of genuine NADases or the residual NADase activity of an ARTase, we purified HvnA and assessed the kinetics of its NADase activity. HvnA had a K_m for NAD$^+$ of 10^{-4} M and a V_{max} of 400 mol of NAD$^+$ consumed/min/mol HvnA (Fig. 7). This V_{max} is 10^2- to 10^4-fold higher than the minor NADase activity reported in certain other bacterial ARTases (15, 39–41). It is also a higher activity than that reported for NADases purified from rabbit erythrocytes and *Bungarus fasciatus* venom, while lower than the activity of NADases purified from *N. crassa* and streptococci (12, 25, 35, 58). Thus, the specific NADase activity of HvnA lies within a range reported for NADases and would be exceptionally high for the background NADase activity of an ARTase.

Symbiosis proficiency of an *hvnA* and *hvnB* double mutant. In order to test possible roles of HvnA and/or HvnB in the *E. scolopes* light organ symbiosis, symbiont-free hatchling squids were inoculated with ES114 and *hvn* mutant strains, and the initiation of symbiosis was monitored. Strains EVS498, EVS499, and EVS500, each successfully infected juvenile *E. scolopes*. The extent of colonization, as measured by luminescence, is equivalent in ES114 and *hvn* mutant-infected animals over 48 h (Fig. 8). In addition, the number of CFUs per light organ is equivalent for ES114 and the *hvnA hvnB* mutant EVS500 (data not shown). Furthermore, when juvenile animals were exposed to low *V. fischeri* inoculum densities, such that only a fraction of inoculated squid became infected, the percentage of animals infected by *hvn* mutants was not significantly different from the percentage infected by wild type (data not shown). SEM analysis revealed that EVS500 triggered regression of the light organ ciliated field in a time frame similar to the regression induced in a wild-type infection. TEM analysis of *E. scolopes* juveniles infected with EVS500 or ES114 similarly revealed no qualitative difference in the morphological effect of infection on host epithelial cells or the spatial pattern of light organ infection by the bacteria.

DISCUSSION

HvnA and HvnB were previously identified as potential signaling molecules in the *V. fischeri-E. scolopes* light organ symbiosis, based on the ability of purified HvnA and HvnB to catalyze polyarginine ribosylation using NAD$^+$ as a substrate, a feature presumptively described as ARTase activity (46, 47). We have demonstrated that the NADase activity of HvnA and HvnB (Fig. 5, 6, and 7) and the subsequent nonenzymatic reaction of free ADPr and polyarginine accounts for the observed HvnA- and HvnB-mediated ADP-ribosylation of polyarginine (Fig. 4). The NADase activity of HvnA displayed a

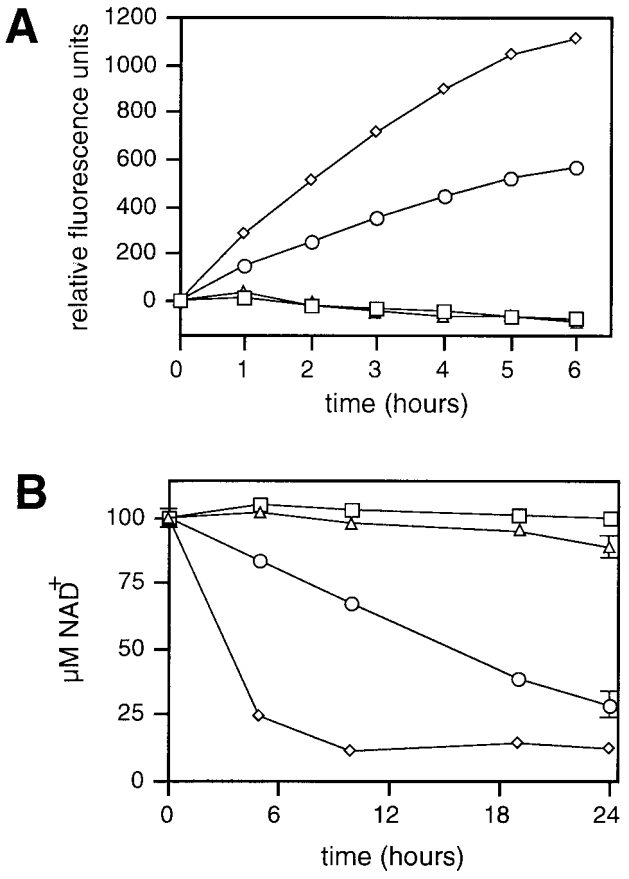

FIG. 5. HvnA and HvnB hydrolysis of ε-NAD^+ and NAD^+. Catalysis of ε-NAD^+ and NAD^+ hydrolysis was measured for cholera toxin (△), HvnA (◇), and HvnB (○). ε-NAD^+ or NAD^+ were added to a 100 μM final concentration. HvnA and HvnB were added as dialyzed preparations of proteins secreted by strains EVS499 and EVS498, respectively. Secreted proteins from strain EVS500 were a negative control (□). Amounts of HvnA, HvnB, and control preparations corresponded to 150 μl of original culture supernatant. A total of 750 ng of cholera toxin was added. Error bars (often too small to visualize) indicate standard errors ($n = 3$). In panel A, the cleavage of ε-NAD^+ is indicated by an increase in the relative fluorescence at 465 nm, when samples were excited at 340 nm. In panel B, NAD^+ was assayed by the addition KCN and measurement of absorbance at 340 nm.

V_{max} (Fig. 7) that was 10^2- to 10^4-fold higher than the minor NADase activity reported in bacterial ARTases such as cholera toxin, pertussis toxin, iota toxin, and exotoxin A (15, 39–41). Consistent with this, the inherent NADase activity of cholera toxin was undetectable in our assays (Fig. 5 and 6), even though cholera toxin catalyzed greater ADP-ribosylation of polyarginine than either HvnA or HvnB (Fig. 4). It remains possible that HvnA and HvnB are ARTases, targeting a specific, as-yet-unknown, host protein, or that some host-derived factor is required to stimulate Hvn ARTase activity. However, neither HvnA nor HvnB have demonstrated bona fide ARTase activity, and the specific activity of NAD^+ hydrolysis by HvnA lies within the range of enzymes categorized as NADases (25, 58). Therefore, based on the available data, we propose that HvnA and HvnB be reclassified as NADases and not as ARTases.

Although ARTases and NADases encompass several distinct protein lineages, three conserved structural motifs have been identified among these families that may be involved in NAD^+ binding and ADPr transfer (43). The new family described here and comprised of HvnA, HvnB, and a putative *P. aeruginosa* protein has conserved regions similar to these motifs that are arranged in the same order (Fig. 2). Region I is comprised of an R or an H residue, often preceded by an aromatic residue and usually followed by a G or A residue (7), a pattern most closely matched by position R113 in the alignment shown in Fig. 2. Region II is a stretch of 13 to 19 amino acids, 20 to 40% of which are aromatic residues, criteria met by positions 147 to 164. Region III is comprised of an active site Q/E-X-E motif, of which the latter E is implicated in NAD^+ hydrolysis in various proteins by cross-linking, site-directed mutagenesis, and crystallographic studies (4, 7, 43, 45). A conserved Q-N-E from positions 276 to 278 in the alignment shown in Fig. 2 could represent this active site motif. It is interesting that although a Q-N-E sequence is found within the alignment of the NADH-utilizing domain of the human nicotinamide nucleotide transhydrogenase with HvnA and HvnB, this conserved E278 residue is not believed to function in

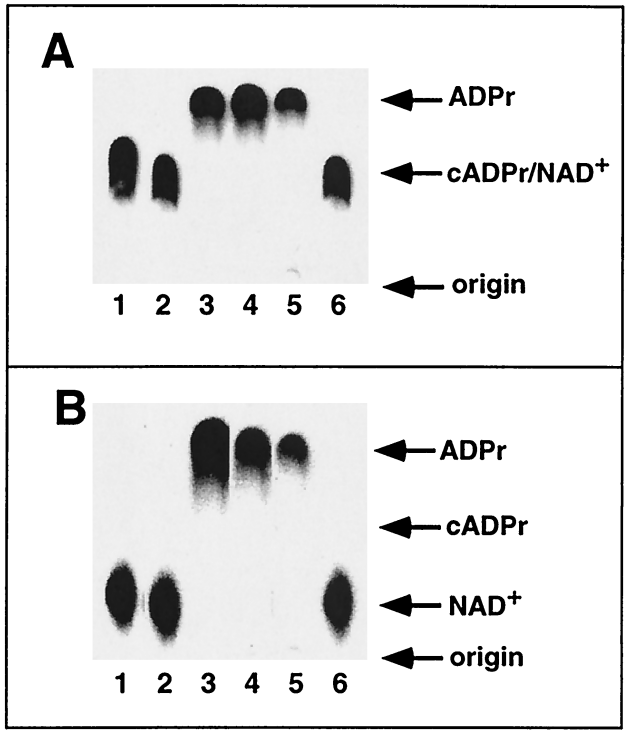

FIG. 6. Product analysis of NAD^+ degradation by TLC. Enzymes were incubated with [^{32}P]NAD^+ in 100-μl reaction volumes, and 5 μl was spotted onto silica TLC plates. After the solvent front had progressed approximately 10 cm, the plates were dried and scored by autoradiography. Lanes 1, 2, and 3 indicate reactions with cholera toxin (75 ng), no enzyme, and *N. crassa* NADase (300 ng), respectively. Lanes 4, 5, and 6 correspond to crude HvnB (secreted proteins from strain EVS498), crude HvnA (secreted proteins from strain EVS499), and a negative control (secreted proteins from strain EVS500), respectively. The mobile phases were H_2O-ethanol-NaCl (A) and H_2O-ethanol-NH_4HCO_3 (B). Arrows mark the mobilities of ADPr or cADPr standards. In panel B, the lanes have been digitally shuffled to match the order in panel A.

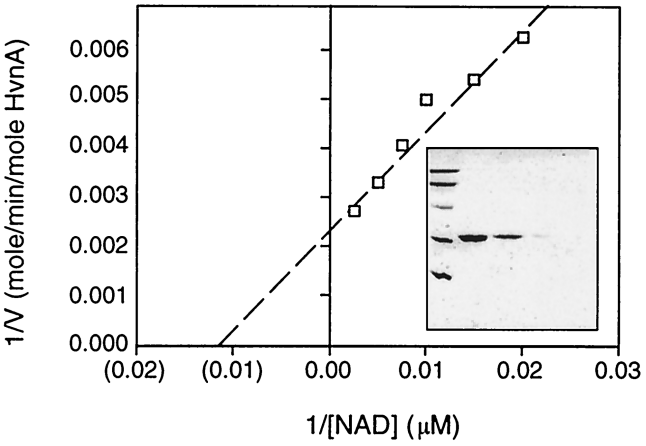

FIG. 7. Kinetics of HvnA NADase activity. Rate of NAD$^+$ degradation was measured in 100-μl reactions with 25 ng of purified HvnA and different concentrations of NAD$^+$. Each velocity measurement was made over a range of data that fit a linear model ($r > 0.9$). The NAD$^+$ concentration was assayed by the addition of KCN, measurement of the absorbance at 340 nm, and comparison to a standard curve. (Inset) SDS-PAGE of (from left): lane 1, 97-, 66-, 45-, 31-, and 21-kDa protein standards; lanes 2 through 5, 6 μg, 3 μg, 600 ng, and 300 ng, respectively, of the purified HvnA used in the above kinetic analyses.

dinucleotide binding in the transhydrogenase family, based on modeling and cross-linking studies (10, 57).

Little is known about secreted bacterial NADases. Clinical streptococcal isolates often secrete NADases (24), and an NADase activity distinct from cholera toxin has been described as an extracellular product of *V. cholerae* (52). Also, an ORF resembling HvnA and HvnB occurs in the *P. aeruginosa* genome, suggesting that this organism may also secrete an NADase. Each of these bacterial species, as well as *V. fischeri*, colonizes the extracellular surface of animal cells, leading us and others (24) to speculate that secretion of NADases may play a role in host colonization or bacterium-animal signaling. NADases could function in animal-bacterium interactions by any of a number of mechanisms.

Secreted bacterial NADases might enable bacteria to use NAD$^+$ as a nutrient in animal tissue; however, using NAD$^+$ as a sole carbon source, strain EVS500 (*hvnA hvnB* mutant) grew at a similar rate and to a similar final density as the wild type (data not shown). NADases could also act essentially like ARTases, mediating a host response via the indirect ribosylation and altered function of a particular host protein (21). Alternatively, if bacterial NADases gained access to host cytoplasm, they could potentially interfere with a number of NAD$^+$-dependent intracellular processes, for example, by inhibiting a respiratory burst response, inducing necrosis, or interfering with signaling by endogenous ARTases, ADPr cyclases, or poly(ADPr) polymerase (18, 28, 56). However, preliminary experiments using immunocytochemistry to localize HvnA in the light organ crypt environment suggest that this NADase does not accumulate inside host cells (A. Small and M. McFall-Ngai, personal communication), arguing against intracellular NAD$^+$ as a primary target.

Although NAD$^+$ has traditionally been thought of as an intracellular metabolite, the discoveries of NAD(H)-metabolizing ectoenzymes anchored to the outer membrane of eukaryotic cells suggest that extracellular NAD$^+$ is important as well. These ectoenzymes include CD38, an ADPr cyclase-cADPr hydrolase (30); PC-1, a nucleotide phosphodiesterase (6); ART-1, an ARTase (29); and a lipoxygenase (42). Both CD38 and ART-1 mediate changes in lymphocyte physiology, and Deterre et al. (6) speculate that NAD$^+$ released from lysing cells may initiate this effect. Secreted bacterial NADases could readily subvert such a signaling system by rapidly degrading extracellular NAD$^+$. Future studies of eukaryotic NAD$^+$-utilizing ectoenzymes and the NADases secreted by animal-associated bacteria will likely be complementary and lead to a better understanding of the role of extracellular NAD$^+$ in animals.

Whatever effect, if any, HvnA and HvnB have on colonization of host tissue may be subtle, considering that mutants defective in one or both *hvn* genes were apparently unaffected in the ability to initiate colonization of the *E. scolopes* light organ and to stimulate apoptotic regression of the light organ ciliated field. The observation that an Hvn homolog appears in *P. aeruginosa*, which like *V. fischeri* establishes long-term chronic colonization in hosts, could intimate that these proteins are involved in persistence, rather than initiation, of infection. Also, although an *hvnA hvnB* mutant triggered observable morphological changes in the light organ in a manner similar to the wild type, these anatomical bacterium-triggered developments may represent only a fraction of the total changes in host cell metabolism and gene expression triggered by *V. fischeri*. A deeper understanding of the interspecies signaling in this symbiosis may help elucidate a symbiotic function for HvnA and HvnB.

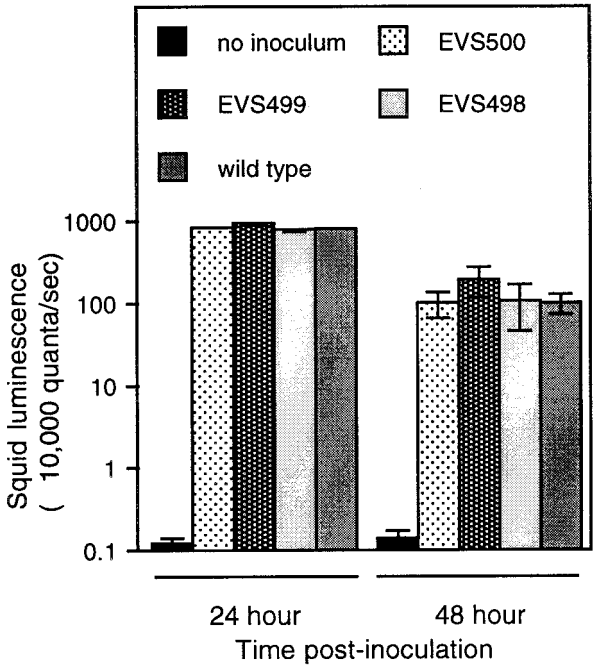

FIG. 8. Colonization of juvenile squid by *V. fischeri* halovibrin mutants. For each treatment, 20 hatchling *E. scolopes* were exposed to 5,000 CFU of *V. fischeri* ml^{-1} or no *V. fischeri* as a control for 3 h and then rinsed with *V. fischeri*-free seawater. Luminescence was measured with a luminometer at 24 and 48 h after inoculation. Error bars indicate the standard errors.

ACKNOWLEDGMENTS

We thank Teresa Biegel, Sonal Dave, Pat Fidopiastis, Jamie Foster, Lynne Gilson, and Todd Vas-Dias for technical assistance; Janice Flory and Margaret McFall-Ngai for insightful comments on the manuscript; and the *Pseudomonas* Genome Project for making their sequence data available.

This work was supported by National Institutes of Health grant RR12294 to E. G. Ruby and M. McFall-Ngai and by National Science Foundation grant IBN-9904601 to M. McFall-Ngai and E. G. Ruby. E.V.S. was supported by a National Research Service Award, F32 GM20041, from the National Institutes of Health.

REFERENCES

1. **Altschul, S. F., W. Gish, W. Miller, E. W. Myers and D. J. Lipman.** 1990. Basic local alignment search tool. J. Mol. Biol. **215:**403–410.
2. **Anderson, B. M., D. A. Yost and C. D. Anderson.** 1986. Snake venom NAD glycohydrolase: purification, immobilization, and transglycosidation. Methods Enzymol. **122:**173–181.
3. **Boettcher, K. J., and E. G. Ruby.** 1990. Depressed light emission by symbiotic *Vibrio fischeri* of the sepiolid squid *Euprymna scolopes*. J. Bacteriol. **172:** 3701–3706.
4. **Carroll, S. F., and R. J. Collier.** 1994. Photoaffinity labeling of active site residues in ADP-ribosylating toxins. Methods Enzymol. **235:**631–639.
5. **Colowick, S. P., N. O. Kaplan and M. M. Ciotti.** 1951. The reaction of pyridine nucleotide with cyanide and its analytical use. J. Biol. Chem. **191:** 447–459.
6. **Deterre, P., L. Gelman, H. Gary-Gouy, C. Arrieumerlou, V. Berthelier, J. M. Tixier, S. Ktorza, J. Goding, C. Schmitt, and G. Bismuth.** 1996. Coordinated regulation in human T cells of nucleotide-hydrolyzing ecto-enzymatic activities, including CD38, and PC-1. Possible role in the recycling of nicotinamide adenine dinucleotide metabolites. J. Immunol. **157:**1381–1388.
7. **Domenighini, M., and R. Rappuoli.** 1996. Three conserved consensus sequences identify the NAD-binding site of ADP-ribosylating enzymes, expressed by eukaryotes, bacteria, and T-even bacteriophages. Mol. Microbiol. **21:**667–674.
8. **Fidopiastis, P. M., S. Von Boletzky, and E. G. Ruby.** 1998. A new niche for *Vibrio logei*, the predominant light organ symbiont of squids in the genus *Sepiola*. J. Bacteriol. **180:**59–64.
9. **Figurski, D. H., and D. R. Helinski.** 1979. Replication of an origin-containing derivative of plasmid RK2 dependent on a plasmid function provided *in trans*. Proc. Natl. Acad. Sci. USA **76:**1648–1652.
10. **Fjellström, O., T. Olausson, X. Hu, B. Källerbring, S. Ahmad, P. D. Bragg, and J. Rydström.** 1995. Three-dimensional structure prediction of the NAD binding site of proton-pumping transhydrogenase from *Escherichia coli*. Proteins **21:**91–104.
11. **Foster, J. S., and M. J. McFall-Ngai.** 1998. Induction of apoptosis by cooperative bacteria in the morphogenesis of host epithelial tissues. Dev. Genes Evol. **208:**295–303.
12. **Grushoff, P. S., S. Shany, and A. W. Bernheimer.** 1975. Purification and properties of streptococcal nicotinamide adenine dinucleotide glycohydrolase. J. Bacteriol. **122:**599–605.
13. **Hagen, T., and M. Ziegler.** 1997. Detection and identification of NAD-catabolizing activities in rat tissue homogenates. Biochim. Biophys. Acta **1340:**7–12.
14. **Haldimann, A., M. K. Prahalad, S. L. Fisher, S.-K. Kim, C. T. Walsh, and B. L. Wanner.** 1996. Altered recognition mutants of the response regulator PhoB: a new genetic strategy for studying protein-protein interactions. Proc. Natl. Acad. Sci. USA **93:**14361–14366.
15. **Han, X. Y., and D. R. Galloway.** 1995. Active site mutations of *Pseudomonas aeruginosa* exotoxin A: analysis of the His^{440} residue. J. Biol. Chem. **270:** 679–684.
16. **Hanahan, D.** 1983. Studies on transformation of *Escherichia coli* with plasmids. J. Mol. Biol. **166:**557–580.
17. **Henikoff, S., and J. G. Henikoff.** 1992. Amino acid substitution matrices from protein blocks. Proc. Natl. Acad. Sci. USA **89:**10915–10919.
18. **Herceg, Z., and Z. Q. Wang.** 1999. Failure of poly(ADP-ribose) polymerase cleavage by caspases leads to induction of necrosis and enhanced apoptosis. Mol. Cell. Biol. **19:**5124–5133.
19. **Herrero, M., V. De Lorenzo, and K. N. Timmis.** 1990. Transposon vectors containing non-antibiotic resistance selection markers for cloning and stable chromosomal insertion of foreign genes in gram-negative bacteria. J. Bacteriol. **172:**6557–6567.
20. **Higashida, H., S. Yokoyama, M. Hashii, M. Taketo, M. Higashida, T. Takayasu, T. Ohshima, S. Takasawa, H. Okamoto, and M. Noda.** 1997. Muscarinic receptor-mediated dual regulation of ADP-ribosyl cyclase in NG108–15 neuronal cell membranes. J. Biol. Chem. **272:**31272–31277.
21. **Hilz, H., R. Koch, W. Fanick, K. Klapproth, and P. Adamietz.** 1984. Nonenzymatic ADP-ribosylation of specific mitochondrial polypeptides. Proc. Natl. Acad. Sci. USA **81:**3929–3933.
22. **Jacobson, E. L., D. Cervantes-Laurean, and M. K. Jacobson.** 1994. Glycation of proteins by ADP-ribose. Mol. Cell. Biochem. **138:**207–212.
23. **Kaniga, K., I. Delor, and G. R. Cornelius.** 1991. A wide-host-range suicide vector for improving reverse genetics in gram-negative bacteria: inactivation of the *blaA* gene of *Yersinia enterocolitica*. Gene **109:**137–141.
24. **Karasawa, T., K. Yamakawa, D. Tanaka, Y. Gyobu, and S. Nakamura.** 1995. NAD^+-glycohydrolase activity of haemolytic streptococci assayed by a simple fluorescent method and its relation to T-serotype. FEMS Microbiol. Lett. **128:**289–292.
25. **Kim, U. H., M. K. Kim, J. S. Kim, M. K. Han, B. H. Park, and H. R. Kim.** 1993. Purification and characterization of NAD glycohydrolases from rabbit erythrocytes. Arch. Biochem. Biophys. **305:**147–152.
26. **Kun, E., A. C. Y. Chang, M. L. Sharma, A. M. Ferro, and D. Nitecki.** 1976. Covalent modification of proteins by metabolites of NAD^+. Proc. Natl. Acad. Sci. USA **73:**3131–3135.
27. **Lamarcq, L. H., and M. J. McFall-Ngai.** 1998. Induction of a gradual, reversible morphogenesis of its host's epithelial brush border by *Vibrio fischeri*. Infect. Immun. **66:**777–785.
28. **Lee, H. C.** 1999. A unified mechanism of enzymatic synthesis of two calcium messengers: cyclic ADP-ribose and NAADP. Biol. Chem. **380:**785–793.
29. **Liu, Z. X., Y. Yu, and G. Dennert.** 1999. A cell surface ADP-ribosyltransferase modulates T cell receptor association and signaling. J. Biol. Chem. **274:**17399–17401.
30. **Lund, F. E., D. A. Cockayne, T. D. Randall, N. Solvason, F. Schuber, and M. C. Howard.** 1998. CD38: a new paradigm in lymphocyte activation and signal transduction. Immunol. Rev. **161:**79–93.
31. **McFall-Ngai, M., C. Brennan, V. Weis, and L. Lamarcq.** 1998. Mannose adhesin-glycan interactions in the *Euprymna scolopes-Vibrio fischeri* symbiosis, p. 273–276. *In* Y. Le Gal and H. O. Halvorson (ed.), New developments in marine biotechnology. Plenum Press, New York, N.Y.
32. **McFall-Ngai, M. J.** 1998. The development of cooperative associations between animals and bacteria: establishing detente among domains. Am. Zool. **38:**593–608.
33. **McFall-Ngai, M. J.** 1998. Pioneering the squid-vibrio model. ASM News **64:**639–645.
34. **McFall-Ngai, M. J., and E. G. Ruby.** 1991. Symbiont recognition and subsequent morphogenesis as early events in an animal-bacterial symbiosis. Science **254:**1491–1494.
35. **Menegus, F., and M. Pace.** 1981. Purification and some properties of NAD-glycohydrolase from conidia of *Neurospora crassa*. Eur. J. Biochem. **113:**485–490.
36. **Miller, J. H.** 1992. A short course in bacterial genetics. Cold Spring Harbor Laboratory Press, Cold Spring Harbor, N.Y.
37. **Montgomery, M. K., and M. J. McFall-Ngai.** 1993. Embryonic development of the light organ of the sepiolid squid *Euprymna scolopes* Berry. Biol. Bull. **184:**296–308.
38. **Montgomery, M. K., and M. J. McFall-Ngai.** 1995. The inductive role of bacterial symbionts in the morphogenesis of a squid light organ. Am. Zool. **35:**372–380.
39. **Moss, J., V. C. Manganiello, and M. Vaughan.** 1976. Hydrolysis of nicotinamide adenine dinucleotide by choleragen and its A protomer: possible role in the activation of adenylate cyclase. Proc. Natl. Acad. Sci. USA **73:**4424–4427.
40. **Moss, J., S. J. Stanley, D. L. Burns, J. A. Hsia, D. A. Yost, G. A. Myers, and E. L. Hewlett.** 1983. Activation by thiol of the latent NAD glycohydrolase and ADP-ribosyltransferase activities of *Bordetella pertussis* toxin (islet-activating protein). J. Biol. Chem. **258:**11879–11882.
41. **Nagahama, M., Y. Sakaguchi, K. Kobayashi, S. Ochi, and J. Sakurai.** 2000. Characterization of the enzymatic component of *Clostridium perfringens* iotatoxin. J. Bacteriol. **182:**2096–2103.
42. **O'Donnell, V. B., and A. Azzi.** 1996. High rates of extracellular superoxide generation by cultured human fibroblasts: involvement of a lipid-metabolizing enzyme. Biochem. J. **318:**805–812.
43. **Okazaki, I. J., and J. Moss.** 1994. Common structure of the catalytic sites of the mammalian and bacterial toxin ADP-ribosyltransferases. Mol. Cell. Biochem. **138:**177–181.
44. **Payne, M. D., E. L. Jacobson, J. Moss, and M. K. Jacobson.** 1985. Modification of proteins by mono-ADP-ribosylation in vivo. Biochemistry **24:**7540–7549.
45. **Radke, J., K. J. Pederson, and J. T. Barbieri.** 1999. *Pseudomonas aeruginosa* exoenzyme S is a biglutamic acid ADP-ribosyltransferase. Infect. Immun. **67:**1508–1510.
46. **Reich, K. A., T. Beigel, and G. K. Schoolnik.** 1997. The light organ symbiont *Vibrio fischeri* possesses two distinct secreted ADP-ribosyltransferases. J. Bacteriol. **179:**1591–1597.
47. **Reich, K. A., and G. K. Schoolnik.** 1996. Halovibrin, secreted from the light organ symbiont *Vibrio fischeri*, is a member of a new class of ADP-ribosyltransferases. J. Bacteriol. **178:**209–215.
48. **Ruby, E. G.** 1996. Lessons from a cooperative bacterial-animal association: the *Vibrio fischeri-Euprymna scolopes* light organ symbiosis. Annu. Rev. Microbiol. **50:**591–624.
49. **Ruby, E. G.** 1999. The *Euprymna scolopes-Vibrio fischeri* symbiosis: a bio-

medical model for the study of bacterial colonization of animal tissue. J. Mol. Microbiol. Biotechnol. **1:**13–21.
50. **Ruby, E. G., and L. M. Asato.** 1993. Growth and flagellation of *Vibrio fischeri* during initiation of the sepiolid squid light organ symbiosis. Arch. Microbiol. **159:**160–167.
51. **Small, A. L., and M. J. McFall-Ngai.** 1998. A halide peroxidase in tissues that interact with bacteria in the host squid *Euprymna scolopes*. J. Cell Biol. **72:**445–457.
52. **Stewart-Tull, E. E., R. A. Ollar, and T. S. Scobie.** 1986. Studies on the *Vibrio cholerae* mucinase complex. I. Enzymatic activities associated with the complex. J. Med. Microbiol. **22:**325–333.
53. **Thompson, J. D., D. G. Higgins, and T. J. Gibson.** 1994. CLUSTAL W: improving the sensitivity of progressive multiple sequence alignment through sequence weighting, positions-specific gap penalties and weight matrix choice. Nucleic Acids Res. **22:**4673–4680.
54. **Visick, K. L., and E. G. Ruby.** 1997. New genetic tools for use in the marine bioluminescent bacterium *Vibrio fischeri*, p. 119–122. *In* J. W. Hastings, L. J. Kricka, and P. E. Stanley (ed.), Bioluminescence and chemiluminescence. John Wiley and Sons, New York, N.Y.
55. **Visick, K. L., and E. G. Ruby.** 1998. The periplasmic, group III catalase of *Vibrio fischeri* is required for normal symbiotic competence and is induced both by oxidative stress and approach to stationary phase. J. Bacteriol. **180:**2087–2092.
56. **Williamson, K. C., and J. Moss.** 1990. Mono-ADP-ribosyltransferases and ADP-ribosylarginine hydrolases: a mono-ADP ribosylation cycle in animals, p. 493–510. *In* J. Moss and M. Vaughan (ed.), ADP-ribosylating toxins and G proteins. American Society for Microbiology, Washington, D.C.
57. **Yamaguchi, M., Y. Hatefi, K. Trach, and J. A. Hoch.** 1988. The primary structure of the mitochondrial energy-linked nicotinamide nucleotide transhydrogenase deduced from the sequence of cDNA clones. J. Biol. Chem. **263:**2761–2767.
58. **Yost, D. A., and B. M. Anderson.** 1981. Purification and properties of the soluble NAD glycohydrolase from *Bungarus fasciatus* venom. J. Biol. Chem. **256:**3647–3653.